Infrared Photodetectors: A Review of Operational Detectors

R. F. Potter and W. L. Eisenman

A comparison is given, in terms of D^*, of the characteristics of most of the photodetectors of both quantum and thermal types, which are available for operational use at the near and intermediate infrared. A discussion of detectors for use at longer wavelengths (up to the mm range) includes two quantum types as well as the cooled bolometers and the pneumatic cell. The review of thermal detectors emphasizes noise limitations as well as spectral characteristics. The need for gray body detectors for use in spectral response measurements is discussed. It is pointed out that a complete noise power spectrum is essential in order to evaluate effectively a detector and determine the operational limitations.

Introduction

Infrared radiation detectors have been the subject of several comprehensive reviews as is needed in a rapidly developing technology. However, the emphasis has been on the class known as quantum photodetectors. With the rapid developments in semiconductor technology in the past decade and a half, an imposing array of such detectors is available for a wide variety of applications. The theory of operation and description of the parameters has an extensive literature.[1] More recently Levinstein and co-workers[2] have given a review of the status of quantum photodetectors including a discussion on the figure of performance known as D^*.

There has been a resurgence of interest in another class of detectors which we call thermal photodetectors, i.e., the detector material absorbs photons and the resulting change in temperature is measured. This is usually detected using an intrinsic property but not always so. An expanding interest in detecting radiation at long wavelengths ($\lambda > 50\ \mu$) has brought about the development of a series of bolometer elements operated at extremely low temperatures ($T < 5.0°$K). There are also a growing number of requirements for detectors capable of operating at considerably higher temperatures (200°K–350°K) and this has given new emphasis to thermistor bolometer elements. It will be the purpose of this review then to emphasize the long-wavelength quantum detectors, to provide recent data on the thermal detectors, to provide a comparison where applicable, and to discuss some special topics in connection with certain parameter measurements that are necessary to provide a quantitative evaluation on a photodetector.

In Table I of Appendix A we list the symbols, definitions, and terms in common use for describing photodetectors and their capabilities. In Appendix A the functional relationships are also given for those figures of performance which are in general modern use in describing photodetectors, including $NEP(P_N)$ and D^*.[3]

Because many detectors have an $A^{-1/2}$ dependence on their detectivity the importance of D^* is that it permits comparison of most detectors of the same type but of different areas.

Note that with D^* or NEP it is not possible to predict the responsivity of any detector of the same type; however, it is possible to predict the signal-to-noise ratio of any detector of the same type. Unfortunately, the manufacture of detectors has not reached the point where this theoretical reproducibility is achieved, and the relationship between different detectors of the same type is complicated by factors that evidently cannot yet be controlled. However, with D^*, an approximation may be made of what is to be expected from different detectors of the same type. For background noise limited detectors, Jones has defined D^{**} which normalizes to unit solid angle.[4] In Figs. 2 and 3 we indicate the detector field of view as well as the operating temperature.

Detailed discussions of the theory of photoconductive, photovoltaic, etc., detectors are available in the literature.[1, 2] Because small signal and noise theory are treated so extensively elsewhere we limit our-

The authors are in the Infrared Division, U.S. Naval Ordnance Laboratory, Corona, California.

Received 6 March 1962.

This work was performed by the Joint Service Infrared Sensitive Element Testing Program at the U.S. Naval Ordnance Laboratory, Corona, California. This program is supported by the Army, Navy, Air Force, and NASA.

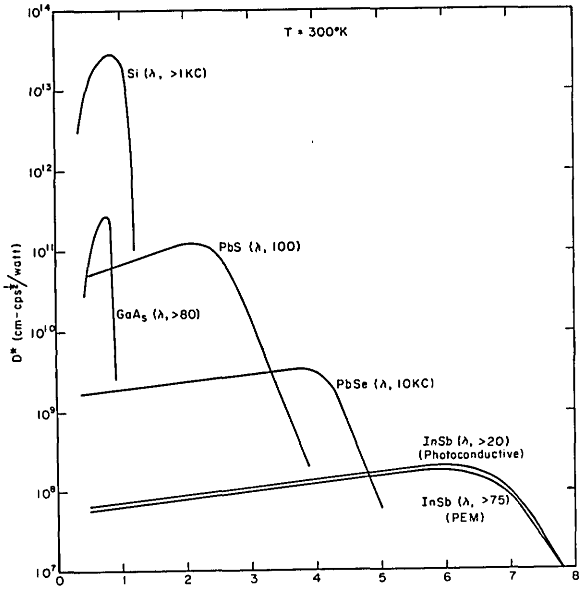

Fig. 1. A comparison of room temperature quantum photodetectors. Parenthesized data indicate spectral data and the optimum operating modulation frequencies. Data are representative of detectors reported in the Photodetector Series Reports, NOLC 474, 527, 557, and 561.

selves to a parametric description. In all the data presented here the measurements are limited in detectivity by the detector noise which in most instances comprises in part or entirely the three noise components described in Appendix B.

Near and Intermediate Infrared Quantum Photodetectors

By quantum photodetectors we mean those devices which operate by photon excitation of an electron state, such an excitation resulting in a detectable change of an intrinsic property, i.e., conduction, electron emission, etc., with the exclusion of a change of temperature. Several classification schemes have been proposed for characterizing detectors in a general way (see R. C. Jones[5]) but we will group detectors according to the operating temperatures. Thus we have four such groups:

(a) 25°C (so-called room temperature)(Fig. 1),
(b) −78°C (so-called dry ice temperature)(Fig. 2),
(c) −196°C (so-called liquid nitrogen temperature) (Fig. 2), and
(d) all lower temperatures (Fig. 3).

Most of these curves are representative of the best detectors which have been measured at Corona, and all detectors of these types are available from commercial sources. Many curves in these figures can be compared with similar curves of 1959[3] and it will be seen that substantial over-all performance improvement has been made. We have also indicated for each respective detector the frequency or the range of frequencies at which the detector can be modulated or "chopped" without reducing its detectivity from optimum.

There are several features out of the ordinary to note in these figures. The room temperature InSb has the same detectivity for the photoconductive as that for the *PEM* mode. Of more general interest are the operating temperature characteristics of the PbS and PbSe film detectors. Each type can be made to peak at or near "dry ice" temperature which is a most important consideration in view of modern cryogenic techniques. Of course if one requires the longer wavelength capabilities he would use a detector designed for operation at a cooler temperature.

Levinstein includes spectral data for several extrinsic germanium detectors in his review.[2]

Long-Wavelength Infrared Quantum Photodetectors

The quantum photodetectors in Fig. 3 which function beyond 7–10 μ are of the impurity photoconductor type, and are semiconductors. The semiconductor absorbs photons of sufficient energy that electrons are excited to the conduction bands and contribute to the conductivity (a similar situation of course holds for hole processes). For operation out to 40 μ these levels

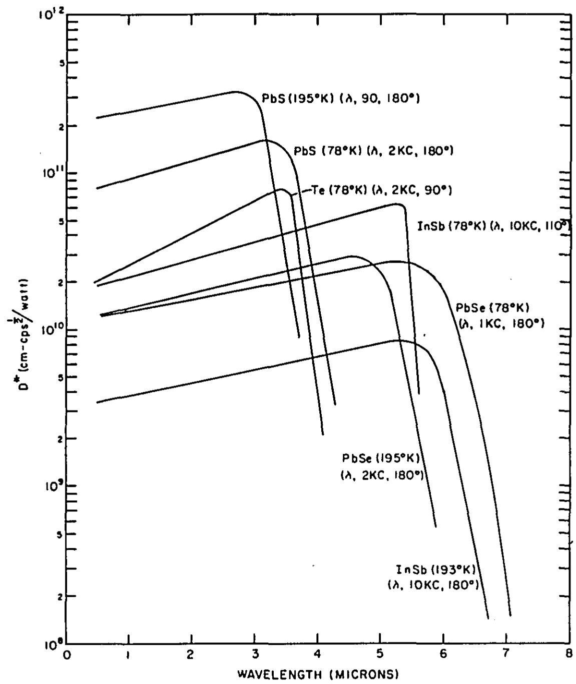

Fig. 2. A comparison of quantum photodetectors operated at dry ice and liquid nitrogen temperatures. The first set of parentheses includes the refrigerant temperature. The second set of parentheses includes an indication of spectral data, optimum modulation frequency, and the field of view in degrees. Data are representative of detectors reported in the Photodetector Series Reports, NOLC 474, 551, 557, and NavWeps 7181.

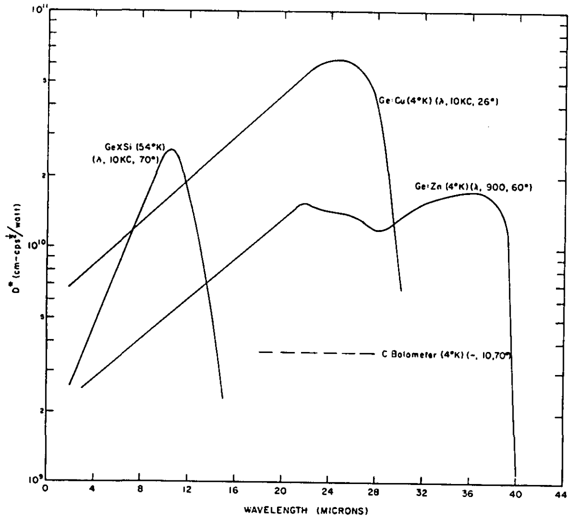

Fig. 3. A comparison of quantum photodetectors operated at $T < 77°K$. The temperatures in parentheses are those of the refrigerants to which the detector heat sink is attached. Spectral characteristics, optimum modulation frequency, and field of view are included in the second set of parentheses. Data are included for a carbon resistor bolometer mounted on a heat sink attached to a 4°K bath in a commercial cryostat. Photodetector Series Reports, NOLC 527 and NavWeps 7181 give further data on the Ge:Cu and the Ge:Si detectors, respectively. The Ge:Zn detector is as reported in ref. 2.

are required to be of the order of 0.03 ev. In order to extend the response to longer wavelengths impurity levels closer to the band must be found.

Putley[6] has described such a detector which can be used in the mm and sub-mm region of the spectrum. The photoconduction is based on the fact that shallow impurity levels are evident in the presence of magnetic fields of strengths, B, *ca* 5000 gauss. These levels appear in relatively pure InSb ($N_0 \simeq 5 \times 10^{13}$ cm^{-3} at 77°K) and have values between 2 and 8×10^{-4} ev.

As can be seen from Fig. 5, there exists an optimum field strength for the effect. Putley suggests that the effect is due to a conventional photoconduction process plus an "electronic bolometer" behavior wherein the radiation is absorbed by the electron gas with a resultant change of mobility. This detector has been used at wavelengths as long as 8 mm. A $D^* = 2 \times 10^{11}$ cm cps$^{1/2}$ watt^{-1} at 1.0 mm was measured in a system considered to be amplifier noise limited.

Another long-wavelength electronic bolometer has been suggested by Goodwin and Jones.[7] Their suggestion is to increase the optical absorption at the cyclotron resonance frequency [$\omega_c = (eB/m^*)$]. This raises the electron gas temperature with a resulting change in conductivity. Measurements on n-type Ge at 4.2°K at $\lambda = 9$ mm, $m^* = 0.13\, m_e$ gave a value of $D^* = 10^{11}$ cm cps$^{1/2}$ watt^{-1}, the detector being Nyquist-Johnson noise limited (see Appendix B). The inventors expect that this could be substantially improved. Whereas the Putley detector has a broad spectral band, the Goodwin-Jones detector has a narrow bandpass. One tunes the center of the bandpass by varying the magnetic field. Detectors of these types, if highly developed, will enable a wholesale exploration of the far infrared spectrum to begin.

Thermal Photodetectors

An excellent source and reference book by Smith *et al.*[8] gives a comprehensive review of all types of thermal photodetectors, including a discussion of the pertinent theory. The present section is limited to a discussion of recent developments.

Thermistor Bolometer

There has been a renewed interest in this type of photoelement, both as a single element and as an array

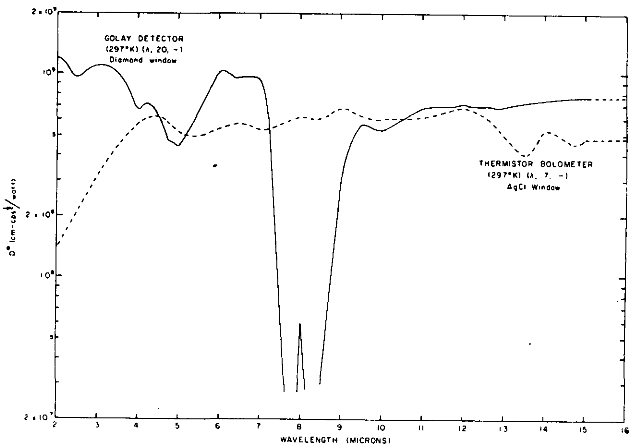

Fig. 4. Spectral detectivity for two thermal photodetectors operated at room temperature. D^* is not a proper figure of performance for the Golay cell, and the values shown here should be multiplied by a factor of 3.6 to give $D = NEP^{-1}$. These data are representative of detectors reported in Photodetector Series Report, NOLC 561.

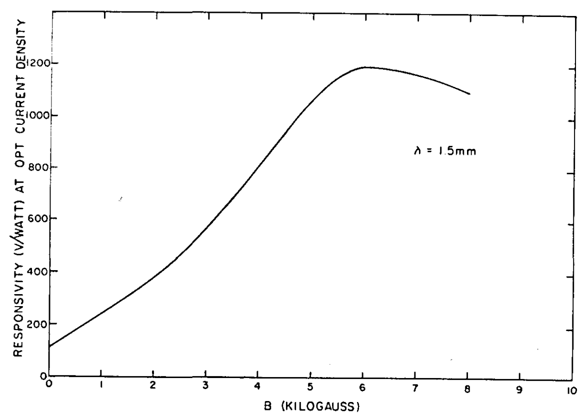

Fig. 5. The responsivity of the Putley detector at $\lambda = 1.5$ mm is shown as a function of the field strength B. The use of a superconductor-wound electromagnet will permit a relatively compact package size. The data given here are taken from that of ref. 6.

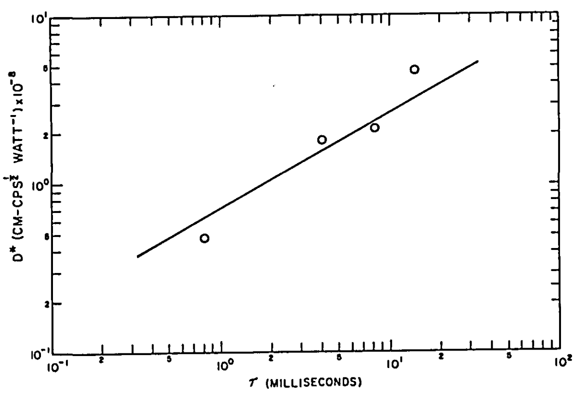

Fig. 6. Optimum detectivity for several thermistor bolometer elements as a function of their response time constant. The four detectors approximately follow the solid line which has a slope of $^1/_2$.

of elements. This interest, of course, stems from their capabilities at longer wavelengths while operating at a temperature near ambient. A spectral curve for D^* is shown in Fig. 4. Thermistor bolometers are among that class of detectors whose D^* exhibits a $\tau^{1/2}$ dependence. In Fig. 6 are shown the detectivities of four such bolometers made up of thermistor material composed of oxidic mixtures of manganese, nickel, and cobalt.[9] It can be seen that one does indeed sacrifice detectivity to obtain a bolometer having a faster response time.

Thermistor bolometers have generally been considered to be limited by the Nyquist-Johnson noise which is frequency independent. Recently, however, improvements in techniques for measuring low-noise power levels at low frequencies have permitted measurements on thermistor bolometers down to 1 cps.[10] In Fig. 7 are shown a family of curves for a bolometer element with a time constant of 8 msec. One can see that an f^{-1} component of noise has set in at 30 cps, and at lower frequencies this type of noise limits the detector. In the same figure are shown a family of curves for $D^*(\lambda_{max})$. One sees that at the higher frequencies the detector is Nyquist-Johnson noise limited.

Cooled Bolometers

The same theoretical conditions hold for bolometers at temperatures other than ambient, the primary considerations being that of thermal conductance and the temperature coefficient of resistivity of the material.

Carbon resistor bolometers and suitably doped germanium elements have been successfully developed for operation at 4.2°K and less.

Carbon composition resistor bolometers operated at 1.5°K have been used extensively by Tinkham and coworkers[11] in their investigation at mm wavelengths. It would be expected that semiconductor bolometers of the type described by Low[12] will come into use in future research at these very long infrared wavelengths. Low estimates that a gallium-doped germanium bolometer operated at 4.2°K with a 180° field of view of 300°K background will be background noise limited and have an NEP of 2.7×10^{-12} watts. Substantial improvements can be achieved by lowering the operating temperature and narrowing the field of view. Selective filtering will also aid in this respect. Low reports that he achieved an NEP of 5×10^{-13} watts operating at 2.15°K with a time constant of 400 μsec. It should be noted that Low's bolometer is operated so that the thermal coupling is through the leads; hence it should have no area dependence.

In reading the literature one cannot but note the variety of conditions under which the low-temperature carbon resistor bolometers have been measured and reported. Boyle and Rodgers[13] report an NEP of 10^{-11} watts for a carbon bolometer operated at 2°K, with an unspecified but evidently very narrow field of view and filtered background radiation. A similar bolometer, fashioned at NOLC, mounted in a commercial liquid helium dewar with a wide field of view and a minimum of filtering, had an NEP of 6×10^{-10} watts when operated at 10 cps. This detector is shown for comparison in Fig. 3 although no spectral measurements were made.

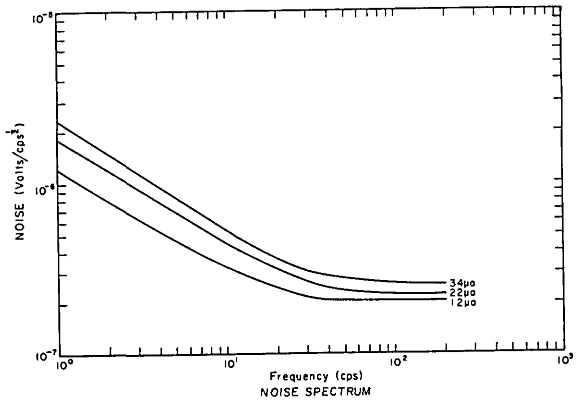

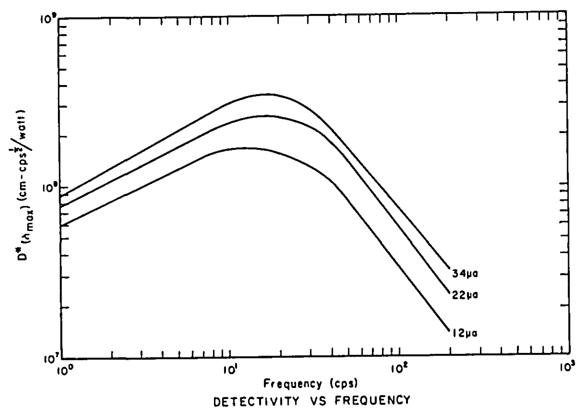

Fig. 7. The low-frequency noise spectrum of a thermistor bolometer is shown in the upper curve. It shows the detector to be f^{-1} noise limited at the lower frequencies. As a result the detectivity peaks at approximately 20 cps.

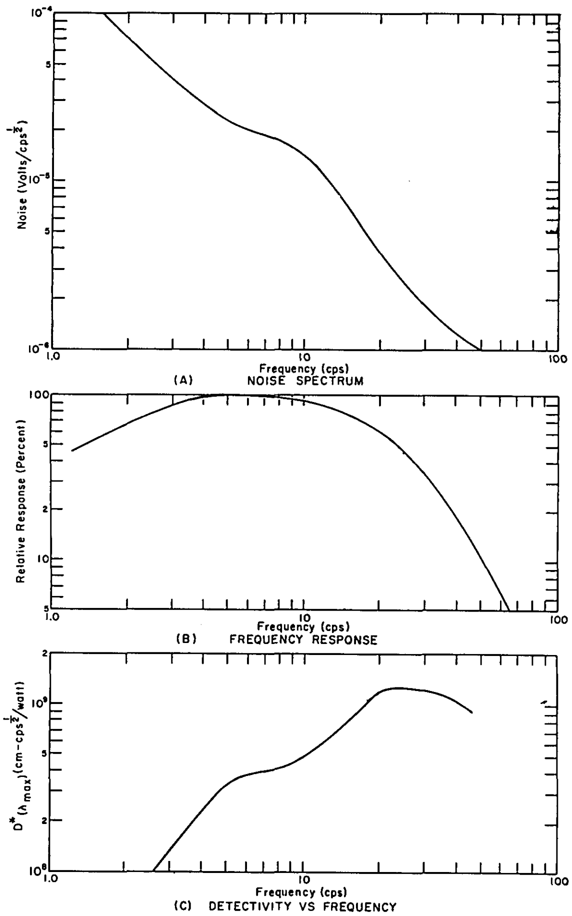

Fig. 8. The low-frequency noise spectrum for a Golay pneumatic detector is shown in the upper curve. The detector is limited by a mixture of the f^{-1} noise of the optical system and response noise. The middle curve shows the effect of ballasting and diaphragm response time on the frequency response. The bottom curve shows the resulting effect on the detectivity. If the detector could be made to be response noise limited, not only would the gouge be eliminated but the detectivity value would be higher.

The authors are not aware of any recent developments for metal strip bolometers and superconducting bolometers; the reader is referred to ref. 8 for a discussion of the known characteristics of these detectors.

Pneumatic Detector

The Golay detector is a widely known detector but somewhat less widely used. There exists an extreme paucity of quantitative information concerning the operating characteristics. In some literature it is described as having a frequency response of the form $r = r_0 (1 + \omega^2\tau^2)^{-1/2}$ which is directly contradictory to the description of the cell operation. Also, many descriptions assume the detector to be response noise limited [Brownian motion of the membrane and power fluctuations (see Appendix B)] with the result that detectivity is expected to have little or no frequency dependence over a wide frequency range. Failure in achieving these conditions, of course, leads (in many instances) to disappointment in the use of the detector.

The Golay cell utilizes the mechanical energy of a pneumatic circuit coupled with an optical system for measuring the mechanical displacement caused by the incoming radiation signal.

In commercial units the optical system operates with a photoemissive tube; thus there are two dominant sources of noise present (Appendix B): (1) The flicker noise (f^{-1}) of the photoemissive cell, and (2) the response noise of the detector.

In order to avoid thermal drift the pneumatic cell is suitably ballasted, resulting in a low-frequency fall-off in the responsivity. There is an additional fall-off occurring at higher frequencies caused by the natural response time of the diaphragm. Apparently no detailed information on these detectors has been made available since the original paper by Golay.[14]

A refurbished detector equipped with a diamond window recently became available for evaluation as it came from the factory. The detectivity as a function of wavelength in the intermediate infrared is shown in Fig. 4 (the strong absorption lines indicate that the window was made from type I diamond). In Fig. 8 are shown the frequency response and noise spectrum. These reflect the presence of thermal ballasting (low-frequency cutoff), natural time constant of the diaphragm, flicker noise of the photocell, and the response noise due to Brownian motion of the diaphragm and power fluctuations. All of these effects are reflected in the frequency spectrum of the detectivity. It is seen that this detector is not quite response-noise limited and that one gains a factor of approximately 2.5 by operating at 20 cps rather than the usual 10 cps. This demonstrates the need of information of the type of Fig. 8 when use of this detector is considered.

Special Considerations

Gray Detectors

Most detectors, as commercially fabricated, have color characteristics due to bulk properties, surface properties, and/or window properties. This becomes a critical problem when one considers the need for a standard gray reference for spectral response measurements. The Golay detector receptor film is hypothetically gray, the film being designed to have a reported impedance of 270 Ω/sq but verification of grayness has evidently never been reported beyond 15 μ. Radiation thermocouples and thermopiles with "blackened" surfaces have long been used as transfer standards. Preliminary measurements carried on at NOLC indicate that the emittances of such surfaces begin to decrease between 10 and 12 μ.

The use of blackened radiation thermocouples as gray body reference standards in the infrared is undoubtedly

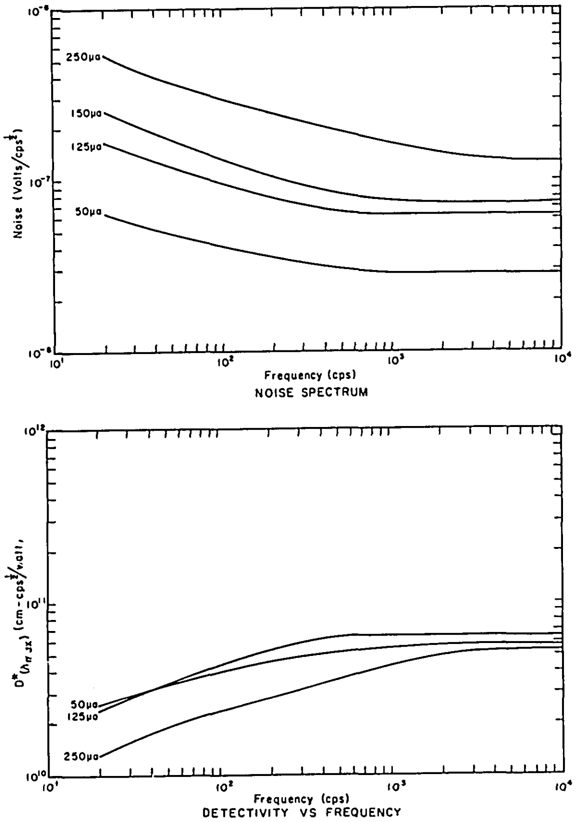

Fig. 9. Frequency spectra of the noise for a liquid nitrogen cooled InSb photoconductor. At higher frequencies the detector is response noise limited (G-R). The detectivity spectra are shown in the lower curve.'

a relatively safe procedure out to wavelengths of approximately 15 μ. However, the unsubstantiated assumption of grayness of these detectors beyond this wavelength may lead to serious difficulties for any extension of radiometry to longer wavelengths.

If the Golay detector is indeed gray, then its use in this connection could be very fruitful over wide spectral ranges, provided one knows the spectral transmittance of the windows used. Parenthetically, several developers of long-wavelength detectors have been using this as a standard. One can find such statements as "the response..." or "the sensitivity is X times that of a Golay detector," but no further reference to the standard is given. The Golay needs further study in this regard, but it may well turn out that, as a standard, it will be a most important link in the radiometric exploration of the far infrared spectrum.

Another approach to this problem has been taken at NOLC. A calorimeter in the shape of a 15° cone, blackened on the inside, total weight 0.25 mg, wall thickness before blackening *ca* 2 μ, has been fabricated and mounted as the receiver for a Bi-BiSn thermocouple. The thermal inertia is such that it can be operated at 1 cps. The geometrical shape and blackening permit a reasonable assumption that this is a black detector. The spectral response of a suitable transfer standard detector (e.g., radiation thermocouple) is compared with that of the assumed blackbody detector. Keeping the transfer standard in the same optical position, the blackbody detector is replaced by the unknown and the spectral comparison made. In this manner, the unknown spectral response can be referred back to that of the blackbody detector. The geometry of the blackbody detector will limit the spectral region for the validity of the blackness assumption.

Although other possibilities suggest themselves, these two detectors seem to be the best available for the near future as gray body standards.

Noise Measurements

Many comparisons of detectors define and use various performance figures which are meant as guides for use by those carrying on detector development. While the user should know and be aware of the limits of the "ideal detector," he cannot rely on *NEP* and D^* alone. These are often given for optimum conditions assuming detector limited conditions only. If he has other empirical information at hand, he may choose to operate the detector in a condition other than "optimum." A case in point is that of the noise characteristics. We have seen how noise departs from the ideal in the case of bolometers and the Golay cell. In Fig. 9 we show the detectivity and noise spectra of a very good photoconductive InSb detector operated at 77°K. Two types of current noise are evident; an f^{-1} component, followed by response noise component (G-R, see Appendix B) for each bias current (at frequencies > 100 Kcps these noise curves would fall off to the Nyquist-Johnson noise level). The optimum bias is 125 μamp but this detector requires an extremely low-noise amplifier to realize this optimum detectivity. From the curves one can determine that by operating at 250 μamp he suffers a 20–30% loss in detectivity but this is offset by being able to relax the noise voltage requirements of his amplifier by a factor of 2.5 or more. Thus there are empirical as well as theoretical reasons for reporting complete pertinent data on detectors. As discussed in Appendix B a complete noise spectrum determines what type of noise is limiting the detector.

The Corona "Detector Series" now reports noise spectra from 1 cps to 10^4 cps (in the pertinent ranges) with a bandpass of 0.3 cps, 1–40 cps and 20 cps–10^4 cps with a 5-cps bandpass for impedances from a few ohms to 100 megohms. Using this capability the noise spectrum of a radiation thermocouple was measured 1 cps to 40 cps, and it was found to be Nyquist-Johnson noise limited down to 1 cps (15-Ω impedance).

Summary

In this review we have attempted to provide a quantitative comparison of most photodetectors in use today (and most are available); these include the intrinsic and extrinsic semiconductor quantum photodetectors as well as several thermal photodetectors. Because of the increasing interest and opportunity in the exploration of the far infrared spectrum by radiometric techniques we have emphasized the recent developments in semiconductor bolometers, and novel far infrared semiconductor detectors. It is our opinion that we will see some most exciting developments in this field (including masers). We have also mentioned two special topics which are generally not covered in detector reviews: (1) Continuing need for standard references for spectral response, and (2) measurement of noise spectra from low to high frequencies.

In conclusion we acknowledge with pleasure the contribution and effort of J. D. Merriam, A. B. Naugle, P. C. Caringella, and R. L. Bates in making the detector evaluation program a success; they are responsible for much of the data drawn upon for this report. We also wish to thank E. H. Putley for furnishing us a preprint of his paper presented before the 1961 International Photoconductivity Conference.

Appendix A

Because the requirements are so diverse, several figures of performance have been developed for use in comparing one detector with others of the same or similar type. The following definitions and functional relationships are given for those which are considered to be the most pertinent in modern day use. They are summarized in Table I.

Responsivity

The responsivity is defined as

$$R = \frac{V}{JA} \frac{\text{volts}}{\text{watts}}. \qquad \text{(A1)}$$

Responsivity, the ratio of the rms value of the fundamental component of the signal voltage to the rms value of the fundamental component of the incident radiation power, is written in functional notation as

$$R = R(b,\lambda,f).$$

The absolute responsivity as a function of wavelength and modulation frequency is given by

$$R(\lambda,f) = R_{bb} \frac{V_\lambda(\lambda)P_{rms}}{V_\lambda(\lambda)P_{\lambda,rms}d\lambda} \frac{V_f(f)}{V_f(f)_r}, \qquad \text{(A2)}$$

where

R_{bb} = responsivity to a blackbody source (or other suitable source having a known spectral content),

f_r = frequency at which R_{bb} is measured,

$P_{rms} = \int_0^\infty P_{\lambda,rms}\, d\lambda$ total rms radiation source power flux.

The term $V_f(f)/V_f(f_r)$ gives the frequency characteristics of the detector, and the term

$$E(P) = \frac{\int_0^\infty V_\lambda(\lambda)P_{\lambda,rms}d\lambda}{P_{rms}} \qquad \text{(A3)}$$

gives the spectral power efficiency; that is, it indicates how effective the detector is compared to a "black" or "gray" detector (detectors with constant response at all wavelengths).

The wavelength dependence of the responsivity can now be written

$$R(\lambda) = \frac{R_{bb}}{E(P)} V_\lambda(\lambda). \qquad \text{(A4)}$$

Since $V_\lambda(\lambda_{max}) = 1$, the term $R_{bb}/E(P)$ gives the maximum response of the detector at the spectral peak.

Noise Equivalent Irradiance

The noise equivalent irradiance is defined as

$$H_N = \frac{NJ}{V(\Delta f)^{1/2}} \frac{\text{watts}}{\text{cps}^{1/2}\ \text{cm}^2}. \qquad \text{(A5)}$$

H_N is the minimum radiant flux density necessary to produce a signal-to-noise ratio of 1 when the noise value is normalized to a unit bandwidth. In functional notation

$$H_N = H_N(b, \lambda, f, A).$$

Since the area of the detector is not taken into account in H_N, the figure describes the performance of a detector of a specific area.

Noise Equivalent Power

The noise equivalent power is defined as

$$NEP = P_N = \frac{NJA}{V(\Delta f)^{1/2}} \frac{\text{watts}}{\text{cps}^{1/2}}. \qquad \text{(A6)}$$

P_N is the minimum radiant flux necessary to produce a signal-to-noise ratio of 1 when the noise value is normalized to unit bandwidth. In functional notation

$$P_N = P_N(b, \lambda, f).$$

D-Star

D-Star, or D^*, is defined as

$$D^* = \frac{A^{1/2}}{P_N} \frac{\text{cm-cps}^{1/2}}{\text{watts}}. \qquad \text{(A7)}$$

D^* is the detectivity normalized to unit area and unit bandwidth. Detectivity is the signal-to-noise ratio produced with unit radiant flux incident on the detector. Since the area dependence of the signal-to-noise ratio has been taken into account, D^* describes the general detector type rather than a detector of some particular area.

In functional notation

$$D^* = D^*(b, \lambda, f).$$

Table I. Figures of Performance

Symbol	Definition in terms of observables	Figures of performance and units
R	$R = V/JA$	Responsivity in volts per watt
NEI	$NEI = JN/V\Delta f^{1/2}$	Noise Equivalent Irradiance in watts/(cm^2 cps$^{1/2}$)
$NEP = P_N$	$NEP = JNA/V\Delta f^{1/2}$	Noise Equivalent Power in watts/cps$^{1/2}$
D^*	$D^* = A^{1/2} (\Delta f)^{1/2}/P_N$	The detectivity normalized to unit area and unit bandwidth in cm-cps$^{1/2}$ watt

Symbol Definitions

A = area of the detector in cm^2,
b = bias applied to the detector,
f = modulation frequency of the radiation incident on the detector,
Δf = frequency bandwidth of the electrical measuring system in cps,
J = radiation flux density in watts/cm^2,
N = noise of the detector in volts,
$P_{\lambda,\text{rms}}$ = rms spectral distribution of radiant power flux,
V = signal of the detector in volts,
$V_b(b)$ = bias dependence of the detector signal,
$V_f(f)$ = frequency dependence of the detector signal,
$V_\lambda(\lambda)$ = spectral dependence of the detector signal,
λ = wavelength, in vacuum, of the radiation incident on the detector.

Appendix B

Fluctuations in the observable parameters or "noise" are what essentially limit the detectivity of detectors. While the several performance figures perform an important and valuable function for comparison and tabulation of large varieties and quantities, the noise power spectrum should be considered no less important. The noise spectra of the detectors included in the report were dominated by some or all of the following three types:

1. $\overline{N^2}_{f^{-1}}\ \alpha\ (i^x/f^y)\Delta f$ where $x = 2$ generally and $y = 1$ although variations from these values have been noted. This noise is commonly called "one over f" noise and is generally attributed to surface effects and faulty contacts.[2]

2. $\overline{N^2}_{\text{N-J}} = 4kTR\Delta f$ where k is the Boltzmann constant, T is absolute temperature, and R is the resistance of circuit. Electrical fluctuations in element occur at thermal equilibrium, hence known as thermal noise, better known as Nyquist-Johnson noise. This type of noise has no frequency dependence except at high frequencies when R should be replaced by the circuit impedance.

3. $\overline{N^2}_r\ \alpha b^x r^2 \Delta f$ where b is an applied bias and r is the detector response. This general type of noise could well be known as signal noise but we prefer to call it response noise because it is caused by fluctuations in the incident radiation or in the fundamental mechanism of the detector and will, therefore, be proportional to responsivity and have the same frequency characteristic [in most cases $r = r_0/(1 + \omega^2 \tau^2)^{1/2}$].

Detectors in the range where they are response noise limited will have a flat detectivity frequency spectrum.

The general class of response noise includes the following:

1. That due to Brownian motion of a diaphragm or similar element.
2. That due to fluctuation in power flowing to and from the sensitive element.
3. Generation-recombination noise (G-R) which includes fluctuation in carrier concentrations caused by emission and absorption of lattice phonons and by absorption of background radiation photons. (If the latter noise is limiting the detector is said to be background limited.)
4. That due to fluctuations in the incident radiation signal (the ultimate limiting noise).

Response noise indicates the fundamental limitation on detectivity for the particular detector considered. When this condition prevails, such action as cooling the lattice, restricting the field of view, or modifying the thermal conductance path etc., can result in performance improvement.

References

1. The reader is referred to "Infrared Issue" Proc. IRE **47**, No. 9 (1959) for several such review articles; P. W. Kruse, L. D. McGlauchlin, R. B. McQuistan, *Elements of Infrared Technology* (John Wiley and Sons, New York, 1962), Chap. 7–10; Proc. Int. Photoconductivity Conference, Ithaca, N.Y. (1961) (in press).
2. P. Bratt, W. Engeler, H. Levinstein, A. MacRae, and J. Pehek, Infrared Physics **1**, 27 (1961).
3. R. C. Jones, Proc. IRE **47**, 1496 (1959).
4. R. C. Jones, J. Opt. Soc. Am. **50**, 1058 (1960); Appl. Opt. **1**, 607 (1962).
5. R. C. Jones, in *Advances in Electronics*, L. Marton, ed. (Academic Press, New York, 1953), Vol. 5, p. 2.
6. E. H. Putley, Proc. Int. Photoconductivity Conference, Ithaca, N.Y. (1961) (in press).
7. D. W. Goodwin and R. H. Jones, J. Appl. Phys. **32**, 2056 (1961).
8. R. A. Smith, F. E. Jones, R. P. Chasmar, *The Detection and Measurement of Infrared Radiation* (Clarendon Press, Oxford, 1957).
9. W. H. Brattain and J. A. Becker, J. Opt. Soc. Am. **46**, 354 (1946).
10. P. C. Caringella and W. L. Eisenman, Rev. Sci. Instr. (in press); "System for Low-Frequency Noise Measurements," NOLC Tech Memo 43-9.
11. P. L. Richards and M. Tinkham, Phys. Rev. **119**, 575 (1960).
12. F. J. Low, J. Opt. Soc. Am. **51**, 1300 (1961).
13. W. S. Boyle and K. F. Rodgers, J. Opt. Soc. Am. **49**, 66 (1959).
14. M. J. E. Golay, Rev. Sci. Instr. **18**, 347, 357 (1947); **20**, 816 (1949).